118 *Organometallics* 1988, *7*, 118–126

Chemical Transformations on Phosphido-Bridged Clusters. Methyne, Methylene Transfer, and Ketene Forming Reactions Involving the μ-Methylene Cluster $Ru_3(CO)_7(\mu\text{-}CH_2)\{\mu_3\text{-}\eta^3\text{-}CH_2{=}C{=}C(i\text{-}Pr)\}(\mu\text{-}PPh_2)$. X-ray Structures of $(\mu\text{-}H)Ru_3(CO)_7\{\mu_3\text{-}\eta^4\text{-}CH{=}C(i\text{-}Pr)C{=}CH_2\}(\mu\text{-}PPh_2)$ and $Ru_3(CO)_6(\mu\text{-}CO)\{\mu_3\text{-}\eta^4\text{-}CH_2{=}C(i\text{-}Pr)C{=}CH_2\}(PPh_3)(\mu\text{-}PPh_2)$

Donato Nucciarone, Nicholas J. Taylor, and Arthur J. Carty*

Guelph-Waterloo Centre for Graduate Work in Chemistry, Department of Chemistry, University of Waterloo, Waterloo, Ontario, Canada N2L 3G1

Antonio Tiripicchio and Marisa Tiripicchio Camellini

Istituto di Chimica Generale, Università di Parma, Centro di Studio per la Strutturistica Diffrattometrica del CNR, Via Massimo d'Azeglio 85, 43100 Parma, Italy

Enrico Sappa

Istituto di Chimica Generale, Università di Torino, Corso Massimo d Azeglio 48, 10125 Torino, Italy

Received April 8, 1987

The μ-methylene cluster $Ru_3(CO)_7(\mu\text{-}CH_2)\{\mu_3\text{-}\eta^3\text{-}CH_2{=}C{=}C(i\text{-}Pr)\}(\mu\text{-}PPh_2)$ (**2**) synthesized from $Ru_3(CO)_8\{\mu_3\text{-}\eta^3\text{-}CH_2{=}C{=}C(i\text{-}Pr)\}(\mu\text{-}PPh_2)$ (**1**) via reaction with diazomethane, CH_2N_2, displays a remarkable reactivity associated with the μ-CH_2 group under mild conditions. Slow isomerization of **2** to the 2-isopropyl-1,3-butadienediyl cluster $(\mu\text{-}H)Ru_3(CO)_7\{\mu_3\text{-}\eta^4\text{-}CH{=}C(i\text{-}Pr)C{=}CH_2\}(\mu\text{-}PPh_2)$ (**3**) [crystal data: triclinic, space group $P\bar{1}$, $a = 9.333$ (2) Å, $b = 10.200$ (1) Å, $c = 16.297$ (2) Å, $\alpha = 87.25$ (1)°, $\beta = 83.26$ (1)°, $\gamma = 64.29$ (1)°, $Z = 2$, $R = 0.025$, $R_w = 0.029$ on 5899 observed reflections] occurs under nitrogen. Cluster **3** contains a triangular Ru_3 core with μ-PPh_2 and μ-H groups on one edge and a four-carbon hydrocarbyl ligand derived from a CH fragment of the μ-methylene bride and the allenyl ligand of **2**. Under an atmosphere of CO and in the presence of methanol complex **2** yields the open allenyl cluster $Ru_3(CO)_9\{\mu_3\text{-}\eta^3\text{-}CH_2{=}C{=}C(i\text{-}Pr)\}(\mu\text{-}PPh_2)$ (**5**) and methyl acetate, both of which were characterized spectroscopically. This reaction is believed to occur via the insertion of CO into the Ru–(μ-methylene) bond to form a C,C-ligated bridging ketenyl intermediate. Treatment of **2** with PPh_3 on the other hand generates the new cluster $Ru_3(CO)_6(\mu\text{-}CO)(PPh_3)\{\mu_3\text{-}\eta^4\text{-}CH_2{=}C(i\text{-}Pr)C{=}CH_2\}(\mu\text{-}PPh_2)$ (**4**) formed by transfer of an intact methylene unit onto the allenyl group of **2**. The structure of **4** was determined crystallographically [crystal data: monoclinic, space group $P2_1/c$, $a = 19.236$ (4) Å, $b = 12.388$ (5) Å, $c = 18.159$ (5) Å, $\beta = 104.66$ (2)°, $Z = 4$, $R = 0.044$, $R_w = 0.058$ based on 4561 observed reflections]. The implications of these reactions for μ-methylene chemistry and for hydrocarbon chain growth on a cluster surface are discussed.

Introduction

Reactions of the cluster-bound C_1 ligands methylidyne, $\equiv$CH, and methylene, $=CH_2$, with other coordinated hydrocarbyls are of interest as molecular models for certain heterogeneous catalytic processes such as the Fischer–Tropsch synthesis.[1] The currently favoured mechanisms of C–C bond formation[2] or hydrogenolysis[3] involve the intermediacy of surface-bound μ-methylenes and their insertion into metal–alkyl bonds or coupling with surface olefins[4] (Scheme I). Other less frequently postulated but plausible pathways implicating μ-CH_2 ligands include the formation of surface vinylidene (or acetylene) from carbide and methylene or vinyl units from methylene and methylidyne fragments. Although there are now numerous examples of binuclear μ-alkylidene complexes which display reactivity modelling surface intermediates,[5,6] fewer reports involving C–C bond formation by coupling of μ-methylene groups and unsaturated hydrocarbyl ligands in

Scheme I. Some Pathways for C–C Coupling Involving μ-Methylene

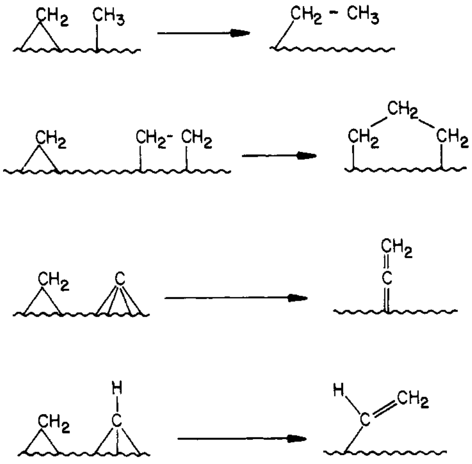

---

(1) For reviews and recent references see: (a) Muetterties, E. L.; Stein, J. *Chem. Rev.* **1979**, *79*, 479. (b) Rofer DePoorter, C. K. *Chem. Rev.* **1981**, *81*, 447. (c) Beanan, L. R.; Keister, J. B. *Organometallics* **1985**, *4*, 1713.

(2) Brady, R. C.; Pettit, R. *J. Am. Chem. Soc.* **1981**, *103*, 1287.

(3) Brady, R. C.; Pettit, R. *J. Am. Chem. Soc.* **1980**, *102*, 6181.

(4) (a) O'Donohue, C.; Clarke, J. K. A.; Rooney, J. J. *J. Chem. Soc., Faraday Trans. 1* **1980**, *76*, 345. (b) Hugues, F.; Besson, B.; Bussière, P.; Dalmon, J. A.; Basset, J. M.; Olivier, D. *Nouv. J. Chim.* **1981**, *5*, 207.

(5) For reviews of μ-methylene complexes see: (a) Herrmann, W. A. *Adv. Organomet. Chem.* **1982**, *20*, 160. (b) Hahn, J. E. *Prog. Inorg. Chem.* **1984**, *31*, 205.

0276-7333/88/2307-0118$01.50/0

polynuclear clusters have appeared.[7,8]

In the previous paper in this series[9] the synthesis of the μ_3-η^3-allenyl cluster $Ru_3(CO)_8\{\mu_3\text{-}\eta^3\text{-}CH_2{=}C{=}C(i\text{-}Pr)\}(\mu\text{-}PPh_2)$ (1) via the coupling of a diazomethane derived methylene group with acetylide ligand in $Ru_3(CO)_6(\mu\text{-}CO)_2\{\mu_3\text{-}\eta^2\text{-}C{\equiv}C(i\text{-}Pr)\}(\mu\text{-}PPh_2)$ was described. Reaction of 1 with a second molecule of diazomethane gives high yields of the μ-methylene cluster $Ru_3(CO)_7(\mu\text{-}CH_2)\{(\mu_3\text{-}\eta^2\text{-}CH_2{=}C{=}C(i\text{-}Pr)\}(\mu\text{-}PPh_2)$ (2) with loss of one molecule of CO.[10] We describe herein some aspects of the remarkable chemical reactivity of 2. Examples of carbon–carbon chain growth via formal transfer of methyne (CH) and methylene (CH_2) units onto the allenyl fragment, the latter promoted by a Lewis base, triphenylphosphine, are discussed. Under carbon monoxide 2 loses the μ-methylene ligand as ketene, which can be trapped as methyl acetate via reaction with methanol, generating the open 50-electron allenyl cluster $Ru_3(CO)_9\{\mu_3\text{-}\eta^3\text{-}CH_2{=}C{=}C(i\text{-}Pr)\}(\mu\text{-}PPh_2)$ (5). These reactions add to a growing body of evidence[8,10] suggesting that μ-CH_2 groups in clusters are versatile, reactive ligands for which a rich chemistry can be anticipated.

Experimental Section

General Procedures, Reagents, and Solvents. All operations and syntheses were performed by using Schlenk techniques. Solvents were stored over an appropriate drying agent and distilled under nitrogen prior to use. Diazomethane was prepared according to standard procedures using Aldrich Chemical Co. *N*-methyl-*N*-nitroso-*p*-toluenesulfonamide.[11] Isotope-enriched $^{13}CH_3OH$ (99.8% ^{13}C) was obtained from MSD Isotopes and ^{13}CO (94.8% ^{13}C) from Monsanto. These were used as received without further purification. Microanalyses were carried out by Guelph Chemical Laboratory. Infrared spectra were measured on Perkin-Elmer 180 and 983 spectrometers using matched NaCl solution cells of 0.5-mm path length. NMR spectra were recorded on Bruker AM-250 (^1H 250 MHz, ^{31}P 101.3 MHz, ^{13}C 62.8 MHz) and WH-400 (^1H 400 MHz, ^{31}P 162.0 MHz, ^{13}C 100.4 MHz) spectrometers. Chemical shifts were referenced to TMS (^1H, ^{13}C) and 85% H_3PO_4 (^{31}P). Lock was provided by the deuteriated solvent.

The synthesis of $Ru_3(CO)_7(\mu\text{-}CH_2)\{\mu_3\text{-}\eta^3\text{-}CH_2{=}C{=}C(i\text{-}Pr)\{(\mu\text{-}PPh_2)$ (2) from the allenyl cluster $Ru_3(CO)_8\{\mu_3\text{-}\eta^3\text{-}CH_2{=}C{=}C(i\text{-}Pr)\}(\mu\text{-}PPh_2)$ has been described in an earlier paper in this series.[9] The deuteriated compounds $Ru_3(CO)_8\{\mu_3\text{-}\eta^3\text{-}CD_2{=}C{=}C(i\text{-}Pr)\}(\mu\text{-}PPh_2)$, $Ru_3(CO)_7(\mu\text{-}CD_2)\{\mu_3\text{-}\eta^3\text{-}CD_2CC(i\text{-}Pr)\}(\mu\text{-}PPh_2)$, and $Ru_3(CO)_7(\mu\text{-}CD_2)\{\mu_3\text{-}\eta^3\text{-}CH_2CC(i\text{-}Pr)\}(\mu\text{-}PPh_2)$ were synthesized from deuteriated diazomethane as follows. KOD was prepared by adding small pieces of solid potassium to D_2O (99.8% ^2H) under a blanket of nitrogen (~0.5 g of K metal in 20 mL). A 10-mL portion of this KOD/D_2O solution was diluted with 10 mL of CH_3CH_2OD (99% CH_3CH_2OD as a 95% solution in D_2O). Deuterium-enriched diazomethane was then prepared and collected by addition of *N*-methyl-*N*-nitroso-*p*-toluenesulfonamide as previously described.[11] This solution was analyzed for deuterium by reacting a freshly prepared solution with ethereal benzoic acid to form methyl benzoate. ^1H NMR was used to quantitate phenyl and methyl protons. 100% ^2H incorporation would give $C_6H_5COOCD_2H$ resulting in a phenyl/methoxy ratio of 5:1. The amount of deuterium enrichment in diazomethane was found to be consistently 85–95%. This CD_2N_2 was used in the preparation of deuteriated 1 and 2 as described.[9]

Reactions of 2. Isomerization to $(\mu\text{-}H)Ru_3(CO)_7\{\mu_3\text{-}\eta^4\text{-}CH{=}C(i\text{-}Pr)C{=}CH_2\}(\mu\text{-}PPh_2)$ (3). Complex 2 was allowed to stand in *n*-heptane solution (3 days at 20 °C or 7 days at 0 °C). The solution was taken to dryness, the solid extracted with CH_2Cl_2 and chromatographed on preparative TLC plates (eluant hexane) affording three bands of which the major component was orange 3. Brown and purple bands contained minor amounts of other products which were not characterized. After recrystallization from heptane the yield of 3 was 25%. IR (C_6H_{12}): (ν(CO) 2066 m, 2033 s, 2014 s, 2004 m, 1983 m, 1950 cm^{-1}. ^{31}P NMR (CD_3COCD_3, –65 °C); δ +184.3. ^{13}C NMR ($CDCl_3$, –60 °C, proton coupled) δ 199–193 (m, CO) 184.1 (s), 149.2 (dd, C(8), $^2J_{PC} = 38$ Hz, $^1J_{CH} = 150$ Hz), 139.4 (d, ipso-CPh, $^1J_{PC} = 25$ Hz), 132.6 (d, ipso-CPh, $^1J_{CP} = 10$ Hz), 133–128 (m, phenyl rings), 120.0 (s), 41.8 (t, C(9), $^1J_{CH} = 164$ Hz), 37.3 (d, C(12), $^1J_{CH} = 129$ Hz), 22.7 (q, CMe, $^1J_{CH} = 127$ Hz), $J_{PH} = 22$ Hz), 22.0 (q, CMe, $^1J_{CH} = 126$ Hz). ^1H NMR (CD_2Cl_2, –70 °C): –18.4 (d, 1 H, $J_{PH} = 22$ Hz), 1.3–1.4 (dd, 6 H, 2.7 (m, 1 H), 4.5 (s, 2 H), 7.0–8.0 (m, 6 H), 8.3 (s, 1 H). Anal. Calcd for $Ru_3PO_7C_{26}H_{21}$: C, 40.05; H, 2.72. Found: C, 39.95; H, 2.78.

Reaction with Triphenylphosphine. Synthesis of $Ru_3(CO)_7(PPh_3)\{\mu_3\text{-}\eta^4\text{-}CH_2{=}C(i\text{-}Pr)C{=}CH_2\}(\mu\text{-}PPh_2)$ (4). To a toluene–heptane (10 mL and 40 mL) solution of 2 (~250 mg, 0.25 mmol) was added 2 equiv of PPh_3 (122 mg, 0.504 mmol), and the mixture was left under nitrogen at 0 °C for 24 h. Column chromatography on Florisil (1:3 benzene–heptane as eluant) revealed four bands: gray, parent cluster; orange, unidentified minor product; yellow, complex 4; red, unidentified minor product. After recrystallization from heptane 4 was obtained in 33% yield. IR (C_6H_{12}): ν(CO) 2032 m, 2013 s, 2001 vs, 1969 m, 1952 m, 1850 w, br cm^{-1} $^{31}P\{^1H\}$ NMR (C_6D_6, 30 °C): δ +35.8 (s, $\mathit{P}Ph_3$), +142.4 (s, μ-$\mathit{P}Ph_2$). ^1H NMR ($CDCl_3$, 30 °C): δ 0.62 (d, $J = 6$ Hz, $C\mathit{H}_3$, 3 H), 1.41 (d, $J = 6$ Hz, $C\mathit{H}_3$, 3 H), 1.51 (m, $J = 6$ Hz, $C\mathit{H}(CH_3)_2$, 1 H), 1.72 (s, $C\mathit{H}_2$, 1 H), 2.17 (s, $C\mathit{H}_2$, 1 H), 2.75 (s, $C\mathit{H}_2$, 1 H), 3.97 (s, $C\mathit{H}_2$, 1 H), 7.02–7.83 (phenyl ring hydrogens). Anal. Calcd for $Ru_3P_2O_7C_{44}H_{36}$: C, 50.72; H, 3.48; P, 5.95. Found: C, 51.10; H, 3.50; P, 6.19.

Reactions of 2 with CO and CH_3OH: ^{13}CO and $^{13}CH_3OH$. Carbon monoxide was bubbled into a Schlenk tube containing 2 (100 mg, 0.12 mmol) and hexane (40 mL) for 3 min. The tube was then sealed and left for 3 days at –5 °C. A color change from black to yellow and the presence of a fluffy, tan precipitate were

---

(6) (a) Sumner, C. E., Jr.; Collier, J. A.; Pettit, R. *Organometallics* **1982**, *1*, 1350. (b) Isobe, K.; Andrews, D. G.; Mann, B. E.; Maitlis, P. E. *J. Chem. Soc., Chem. Commun.* **1981**, 809. (c) Herrmann, W. A.; Plank, J.; Riedel, D.; Ziegler, M. L.; Weidenhammer, K.; Guggolz, E.; Balbach, B. *J. Am. Chem. Soc.* **1981**, *103*, 63. (d) Hursthouse, M. B.; Jones, R. A.; Abdul Malik, K. M.; Wilkinson, G. *Ibid.* **1979**, *101*, 4128. (e) Theopold, K. H.; Bergman, R. G. *Ibid.* **1981**, *103*, 2489. (f) Theopold, K. H.; Bergman, R. G. *J. Am. Chem. Soc.* **1983**, *105*, 464. (g) Motyl, K. M.; Norton, J. R.; Schauer, C. K.; Anderson, O. P. *J. Am. Chem. Soc.* **1982**, *104*, 7325. (h) Davies, D. L.; Knox, S. A. R.; Mead, K. A.; Morris, M. J.; Woodward, P. *J. Chem. Soc., Dalton Trans.* **1984**, 2293. (i) Colborn, R. E.; Dyke, A. F.; Knox, S. A. R.; MacPherson, K. A.; Orpen, A. G. *J. Organomet. Chem.* **1982**, *239*, C15. (j) Dyke, A. F.; Knox, S. A. R.; Naish, P. J.; Taylor, G. E. *J. Chem. Soc., Chem. Commun.* **1980**, *803*. (k) Cooke, M.; Davies, D. L.; Guerchais, J. E.; Knox, S. A. R.; Mead, K. A.; Roué, J.; Woodward, P. *Ibid.* **1981**, 862. (l) Colborn, R. E.; Dyke, A. F.; Knox, S. A. R.; Mead, K. A.; Woodward, P. *J. Chem. Soc., Dalton Trans.* **1983**, 2099 and earlier papers in this series. (m) Levisalles, J.; Rose-Munch, F.; Rudler, H.; Daran, J.-C.; Dromzee, Y.; Jeannin, Y. *J. Chem. Soc., Chem. Commun.* **1980**, *685*. (n) Levisalles, J.; Rose-Munch, F.; Rudler, H.; Daran, J. C.; Jeannin, Y. *J. Chem. Soc., Chem. Commun.* **1981**, *1057*. (o) Rudler, H. *J. Mol. Catal.* **1980**, *8*, 53. (p) Azam, K. A.; Frew, A. A.; Lloyd, B. R.; Manojlovic-Muir, L.; Muir, K. W.; Puddephatt, R. J. *J. Chem. Soc., Chem. Commun.* **1982**, *614*. (q) Okeya, S.; Meanwell, N. J.; Taylor, B. F.; Isobe, K.; Vazquez de Miguel, A.; Maitlis, P. M. *J. Chem. Soc., Dalton Trans.* **1984**, 1453. (r) Isobe, K.; Okeya, S.; Meanwell, N. J.; Smith, A. J.; Adams, H.; Maitlis, P. M. *J. Chem. Soc., Dalton Trans.* **1984**, 1215. (s) Isobe, K.; Vasquez de Miguel, A.; Nutton, A.; Maitlis, P. M. *J. Chem. Soc., Dalton Trans.* **1984**, 929.

(7) (a) Shapley, J. R.; Sievert, A. C.; Churchill, M. R.; Wassermann, H. *J. Am. Chem. Soc.* **1981**, *103*, 6975. (b) Clauss, A. D.; Shapley, J. R.; Wilson, S. R. *J. Am. Chem. Soc.* **1981**, *103*, 7387.

(8) For a selection of recent references to μ-methylene cluster chemistry see: (a) Dimas, P. A.; Duesler, E. N.; Lawson, R. J.; Shapley, J. R. *J. Am. Chem. Soc.* **1980**, *102*, 7787. (b) Herrmann, W. A.; Plank, J.; Guggolz, E.; Ziegler, M. L. *Angew. Chem., Int. Ed. Engl.* **1980**, *19*, 651. (c) Sievert, A. C.; Strickland, D. S.; Shapley, J. R.; Steinmetz, G. R.; Geoffroy, G. L. *Organometallics* **1982**, *1*, 214. (d) Morrison, E. D.; Steinmetz, G. R.; Geoffroy, G. L.; Fulz, W. C.; Rheingold, A. L. *J. Am. Chem. Soc.* **1984**, *106*, 4783. (e) Holmgren, J. S.; Shapley, J. R., *Organometallics* **1984**, *3*, 1322. (f) Morrison, E. D.; Geoffroy, G. L.; Rheingold, A. L. *J. Am. Chem. Soc.* **1985**, *107*, 254. (g) Holmgren, J. S.; Shapley, J. R. *Organometallics* **1985**, *4*, 793. (h) Farrugia, L. J.; Green, M.; Hankey, D. A.; Murray, M.; Orpen, A. G.; Stone, F. G. A. *J. Chem. Soc., Dalton Trans.* **1985**, 177. (i) Adams, R. D.; Babin, J. E.; Tasi, M. *Organometallics* **1986**, *5*, 1920.

(9) Nucciarone, D.; Taylor, N. J.; Carty, A. J. *Organometallics*, first of three papers in this issue.

(10) Preliminary communication: Nucciarone, D.; Taylor, N. J.; Carty, A. J. *Organometallics* **1984**, *3*, 177.

(11) (a) DeBoer, T. J.; Backer, H. J. *Org. Synth.* **1956**, *36*, 16. (b) Black, T. H. *Aldrichim. Acta* **1983**, *16*, 3.

Table I. Experimental Details of X-ray Data Collection, Reduction, and Refinement for 3 and 4

	3	4
formula	$Ru_3PO_7C_{26}H_{21}$	$Ru_3P_2O_7C_{44}H_{36}$
mol wt	779.64	1041.92
cryst system	triclinic	monoclinic
space group	$P\bar{1}$	$P2_1/c$
a, Å	9.333 (2)	19.236 (4)
b, Å	10.200 (1)	12.388 (5)
c, Å	16.297 (2)	18.159 (5)
α, deg	87.25 (1)	
β, deg	83.26 (1)	104.66 (2)
γ, deg	64.29 (1)	
V, Å^3	1388.2 (4)	4186 (2)
Z	2	4
D_{calcd}, g·cm^{-3}	1.865	1.653
μ(Mo Kα), cm^{-1}	16.72	11.71
cryst size, mm	0.25 × 0.29 × 0.29	0.14 × 0.23 × 0.51
diffractometer	Syntex $P2_1$	Siemens AED
radiation (λ, Å)	graphite-monochromated Mo Kα (0.71069)	Nb-filtered Mo Kα (0.71069)
scan type	$\theta/2\theta$	$\theta/2\theta$
scan speed, deg min^{-1}	2.5–29.3	3–12
scan width, deg	0.8 below Kα_1 to 0.8 above Kα_2	$(\theta - 0.5) - [\theta + (0.5 + \Delta\theta)][\Delta\theta = \{\lambda_{\alpha2} - \lambda_{\alpha1})/\gamma\} \tan\theta]$
2θ range, deg	3–50	6–50
std reflcns	2 after every 10 measurements	1 after every 50 measurements
unique total data	6760	7352
obsd data	5899 ($I \geq 3\sigma(I)$)	4561 ($I \geq 2\sigma(I)$)
R	0.025	0.044
R_w	0.029	0.058
final diff map electron density, e·Å^{-3}	0.5	0.62

noted. IR examination revealed only the presence of $Ru_3(CO)_9\{\mu_3\text{-}\eta^3\text{-}CH_2{=}C{=}C(i\text{-}Pr)\}(\mu\text{-}PPh_2)$ (**5**),[9] the starting material **2** having completely disappeared.

Removal of the CO atmosphere and purging with N_2 resulted in a color change from yellow to maroon as a result of decarbonylation of **5** to give the allenyl complex **1**. After 3 h, workup via fractional crystallization gave a total recovery of **1** of 72 mg (72%).

To a 250-mL three-necked flask containing **2** (100 mg, 0.12 mmol) in heptane (30 mL) was added methanol (2 equiv). The N_2 atmosphere was replaced with CO and the system stirred at room temperature for 4 h and then frozen in liquid nitrogen. The system was evacuated and allowed to warm to room temperature. Under a static vacuum part of the solution was distilled into Schlenk tubes on the vacuum line and the distillates were frozen in liquid nitrogen. IR and NMR analyses were carried out on the samples. Similar procedures were employed by using ^{13}CO and $^{13}CH_3OH$.

X-ray Crystal Structure Analyses. $(\mu\text{-}H)Ru_3(CO)_7\{\mu_3\text{-}\eta^4\text{-}CH{=}C(i\text{-}Pr)C{=}CH_2\}(\mu\text{-}PPh_2)$ (3). Preliminary X-ray examination of yellow prisms of **3** (from n-heptane) mounted on a glass fiber, indicated no systematic absences and Laue symmetry no higher than C_i—$\bar{1}$. The data crystal selected for intensity measurements had dimensions of 0.25 × 0.29 × 0.29 mm, and accurate unit cell parameters were obtained from refinement of the setting angles for 15 reflections well dispersed in reciprocal space, using the Syntex $P2_1$ autoindexing and cell refinement routines. Crystal data and further details of the collection, reduction, and refinement of X-ray data are given in Table I. Data were corrected for Lorentz and polarization effects but not for absorption.

The structure was solved by the heavy-atom method, the ruthenium and phosphorus atoms being located in a sharpened Patterson function and the remaining atoms in subsequent Fourier syntheses. Refinement of positions and isotropic thermal parameters for all 37 non-hydrogen atoms gave an R value ($R = \sum|F_o| - |F_c|/\sum|F_o|$) of 0.064. Conversion to anisotropic coefficients followed by several cycles of least-squares analysis gave convergence at $R = 0.033$. A difference Fourier synthesis then revealed reasonable positions for all of the hydrogen atoms in the structure. In subsequent cycles of refinement these were included, positions and isotropic temperature factors being refined. Introduction of an appropriate weighting scheme (Table I) and refinement to convergence gave $R = 0.025$ with R_w ($R_w = [\sum_w(|F_o| - |F_o|)^2/\sum_w(|F_o|)^2]^{1/2}$) = 0.029. The final difference map was featureless with maximum electron density at the level of 0.5 e Å^{-3}. Scattering factors used including corrections for the real and imaginary components of anomalous dispersion for the heavy atoms were taken from ref 12. Hydrogen atom scattering factors were those of Stewart et al.[13] All calculations were carried out on linked IBM 4341 systems in the University of Waterloo, Department of Computer Services. Tables II and III contain listings of atomic coordinates and important bond lengths and angles. Thermal parameters (Table S1), remaining bond lengths and angles (Table S2), and structure factors (Table S3) have been deposited as supplementary material.

$Ru_3(CO)_6(\mu\text{-}CO)(PPh_3)\{\mu_3\text{-}\eta^4\text{-}CH_2{=}C(i\text{-}Pr)C{=}CH_2\}(\mu\text{-}PPh_2)$ (4). Crystals of **4** suitable for the X-ray analysis were obtained by slow cooling of heptane solutions of the complex at −5 °C.

A red-orange prismatic crystal was selected and mounted on a Siemens AED diffractometer. Crystal data and data collection parameters are given in Table I. Unit cell parameters were obtained by least-squares refinement of the 2θ values of 30 carefully centered reflections (with θ in the range 10–15°).

Data were collected at room temperature, the individual reflection profiles having been analyzed by the method of Lehmann and Larsen.[15] Structure amplitudes were obtained in the usual way following the application of Lorentz and polarization corrections. No absorption correction was deemed necessary. Only observed reflections ($I \geqslant 2\sigma(I)$) were used in the solution and refinement.

The structure was solved by direct and Fourier methods and refined by full-matrix least-squares techniques first with isotropic and then with anisotropic thermal parameters for the Ru, P, O, and C(1)–C(14) atoms. All of the hydrogen atoms were located in a final difference Fourier map; these were included in the final structure factor calculations with fixed isotropic thermal parameters ($B = 7.0$ Å^2). The function minimized during the refinement was $\sum w|\Delta F|^2$. The weighting scheme used in the last cycles was $w = K/[\delta^2(F_o) + gF_o^{\,2}]$. At convergence the values for K and g were 0.8378 and 0.005, respectively. The final R and R_w values were 0.044 and 0.058 ($R = \sum(|F_o| - F_c|)/\sum|F_o|$ and $R_w = [\sum w(|F_o| - |F_c|)^2/\sum w|F_o|^2]^{1/2}$. A final difference map was featureless. Scattering factors used were taken from tabulations in ref 12, with the exception of those of the hydrogen atoms which were taken from ref 13. Corrections for the real and imaginary components of anomalous dispersion were made for the Ru and P atoms. Data reduction, structure solution, and refinement were carried out on a Cyber 7600 computer at the Centro di Calcolo dell'Italie Nord-Orientale, Bologna, using the SHELX-76 system of computer programs. Atomic coordinates are listed in Table IV and important bond lengths and angles in Table V. Anisotropic thermal parameters (Table S4), remaining bond lengths and angles (Table S5), and structure factors (Table S6) have been deposited.

Results and Discussion

Reactions of the μ-Methylene Cluster 2. The reaction sequence illustrated in Scheme II leads to the synthesis of the μ-methylene complex **2** in workable overall

---

(12) *International Tables for X-ray Crystallography*; Kynoch: Birmingham, 1974; Vol. IV.

(13) Stewart, R. F.; Davidson, E. R.; Simpson, W. T. *J. Chem. Phys.* **1965**, *42*, 3175.

(14) Carty, A. J.; Mott, G. N.; Taylor, N. J.; Yule, J. E. *J. Am. Chem. Soc.* **1978**, *100*, 3051.

(15) Lehman, M. S.; Larsen, F. K. *Acta Crystallogr., Sect. A: Cryst. Phys., Diffr. Theor. Gen. Crystallogr.* **1974**, *A30*, 580.

Table II. Atomic Coordinates (Fractional × 10^4) and Hydrogen Atom Thermal Parameters for (μ-H)$Ru_3(CO)_7${μ_3-η^4-CH=C(*i*-Pr)C=CH_2}(μ-PPh_2) (3)

(a) Heavy Atoms

atom	*x*	*y*	*z*
Ru(1)	1588.8 (2)	598.2 (2)	3280.7 (1)
Ru(2)	1982.6 (3)	−38.3 (2)	1512.1 (1)
Ru(3)	4266.3 (2)	500.1 (2)	2321.1 (1)
P	2343.7 (8)	2507.7 (7)	3051.7 (4)
O(1)	1645 (4)	414 (4)	5119 (2)
O(2)	−2011 (3)	2439 (3)	3572 (2)
O(3)	3018 (4)	1475 (4)	55 (2)
O(4)	832 (5)	−1595 (4)	393 (2)
O(5)	−1307 (4)	2508 (4)	1650 (2)
O(6)	5796 (4)	1641 (4)	914 (2)
O(7)	7215 (3)	−171 (4)	3134 (2)
C(1)	1621 (4)	505 (4)	4422 (2)
C(2)	−681 (4)	1734 (3)	3447 (2)
C(3)	2658 (4)	919 (4)	601 (2)
C(4)	1265 (5)	−1023 (4)	809 (2)
C(5)	−75 (4)	1565 (4)	1627 (2)
C(6)	5187 (4)	1209 (4)	1434 (2)
C(7)	6089 (4)	96 (4)	2831 (2)
C(8)	4562 (3)	−1417 (3)	1784 (2)
C(9)	1231 (4)	−1539 (3)	3234 (2)
C(10)	2140 (3)	−1352 (3)	2556 (2)
C(11)	3650 (3)	−2170 (3)	2072 (2)
C(12)	3995 (4)	−3706 (3)	1820 (2)
C(13)	4852 (5)	−4744 (4)	2495 (3)
C(14)	4970 (8)	−4182 (5)	984 (3)
C(15)	2760 (4)	3227 (3)	3956 (2)
C(16)	3830 (5)	2263 (4)	4468 (2)
C(17)	4232 (6)	2762 (6)	5145 (3)
C(18)	3570 (6)	4218 (5)	5316 (2)
C(19)	2519 (6)	5171 (5)	4825 (2)
C(20)	2104 (5)	4690 (4)	4149 (2)
C(21)	992 (3)	4102 (3)	2526 (2)
C(22)	−510 (4)	5045 (4)	2902 (3)
C(23)	−1524 (5)	6229 (4)	2484 (3)
C(24)	−1066 (6)	6493 (5)	1685 (4)
C(25)	386 (6)	5572 (5)	1301 (3)
C(26)	1422 (4)	4380 (4)	1718 (2)

(b) Hydrogen Atoms

atom	*x*	*y*	*z*	U_{iso}, Å^2
H(1)	360 (5)	−34 (5)	313 (3)	73 (9)
H(8)	538 (4)	−194 (3)	133 (2)	36 (9)
H(9A)	181 (4)	−224 (4)	366 (4)	52 (9)
H(9B)	9 (5)	−114 (4)	326 (2)	55 (9)
H(12)	297 (4)	−369 (4)	180 (2)	41 (10)
H(13A)	494 (5)	−566 (5)	237 (3)	76 (13)
H(13B)	428 (5)	−443 (5)	303 (3)	69 (12)
H(13C)	586 (6)	−477 (5)	251 (3)	77 (12)
H(14A)	503 (6)	−509 (5)	87 (3)	82 (14)
H(14B)	459 (6)	−362 (5)	57 (3)	84 (14)
H(14C)	604 (7)	−439 (6)	102 (3)	98 (15)
H(16)	433 (5)	134 (4)	437 (2)	59 (14)
H(17)	483 (6)	209 (5)	542 (3)	86 (15)
H(18)	387 (6)	444 (5)	574 (3)	91 (14)
H(19)	200 (5)	621 (5)	499 (3)	77 (14)
H(20)	136 (5)	539 (4)	383 (2)	59 (12)
H(22)	−75 (5)	487 (4)	342 (2)	56 (13)
H(23)	−255 (5)	688 (4)	275 (2)	61 (14)
H(24)	−174 (6)	729 (6)	138 (3)	102 (15)
H(25)	70 (4)	568 (4)	80 (2)	53 (14)
H(26)	233 (5)	382 (4)	149 (2)	51 (13)

Table III. Important Bond Lengths (Å) and Angles (deg) for (μ-H)$Ru_3(CO)_7${μ_3-η^4-CH=C(*i*-Pr)C=CH_2}(μ-PPh_2) (3)

(a) Bond Lengths

Ru(1)–Ru(2)	2.9306 (2)	Ru(1)–Ru(3)	2.7534 (2)
Ru(2)–Ru(3)	2.8856 (3)	Ru(1)–P	2.3427 (7)
Ru(3)–P	2.3184 (6)	Ru(1)–C(1)	1.860 (3)
Ru(1)–C(2)	1.915 (3)	Ru(2)–C(3)	1.931 (4)
Ru(2)–C(4)	1.908 (4)	Ru(2)–C(5)	1.902 (4)
Ru(3)–C(6)	1.870 (4)	Ru(3)–C(7)	1.856 (4)
Ru(1)–C(9)	2.350 (3)	Ru(1)–C(10)	2.193 (3)
Ru(2)–C(8)	2.285 (3)	Ru(2)–C(10)	2.094 (3)
Ru(2)–C(11)	2.278 (3)	Ru(3)–C(8)	2.075 (3)
Ru(1)–H(1)	1.69 (5)	Ru(3)–H(1)	1.74 (5)
P–C(15)	1.830 (3)	P–C(21)	1.819 (3)
C(1)–O(1)	1.138 (4)	C(2)–O(2)	1.131 (4)
C(3)–O(3)	1.128 (5)	C(4)–O(4)	1.129 (6)
C(5)–O(5)	1.132 (6)	C(6)–O(6)	1.143 (5)
C(7)–O(7)	1.133 (5)	C(8)–(11)	1.405 (4)
C(9)–C(10)	1.369 (5)	C(10)–C(11)	1.444 (4)
C(11)–C(12)	1.524 (4)	C(12)–C(13)	1.526 (5)
C(12)–C(14)	1.520 (6)		

(b) Bond Angles

Ru(2)–Ru(1)–Ru(3)	60.93 (1)		
Ru(1)–Ru(2)–Ru(3)	56.50 (1)		
Ru(1)–Ru(3)–Ru(2)	62.57 (1)		
Ru(1)–P–Ru(3)	72.41 (1)	Ru(1)–P–C(15)	116.8 (1)
Ru(1)–P–C(21)	116.5 (1)	Ru(3)–P–C(15)	122.3 (1)
Ru(3)–P–C(21)	121.4 (1)	C(15)–P–C(21)	105.0 (1)
Ru(1)–C(1)–O(1)	178.3 (1)	Ru(1)–C(2)–O(2)	176.9 (1)
Ru(2)–C(3)–O(3)	177.9 (1)	Ru(2)–C(4)–O(4)	179.5 (2)
Ru(2)–C(5)–O(5)	176.2 (2)	Ru(3)–C(6)–O(6)	177.1 (1)
Ru(3)–C(7)–O(7)	178.8 (1)	Ru(2)–C(8)–Ru(3)	82.7 (0)
Ru(2)–C(8)–C(11)	71.8 (1)	Ru(3)–C(8)–C(11)	122.7 (1)
Ru(1)–C(9)–C(10)	66.3 (1)	Ru(1)–C(10)–Ru(2)	86.2 (0)
Ru(1)–C(10)–C(9)	78.9 (1)	Ru(1)–C(10)–C(11)	124.5 (1)
Ru(2)–C(10)–C(9)	141.8 (1)	Ru(2)–C(10)–C(11)	77.8 (1)
C(9)–C(10)–C(11)	139.0 (1)	Ru(2)–C(11)–C(8)	78.3 (1)
Ru(2)–C(11)–C(10)	63.9 (1)	Ru(2)–C(11)–C(12)	127.3 (1)
C(8)–C(11)–C(10)	117.1 (1)	C(8)–C(11)–C(12)	125.6 (1)
C(10)–C(11)–C(12)	116.7 (1)	C(11)–C(12)–C(13)	107.9 (1)
C(11)–C(12)–C(14)	114.1 (2)	C(13)–C(12)–C(14)	110.5 (2)

Scheme II

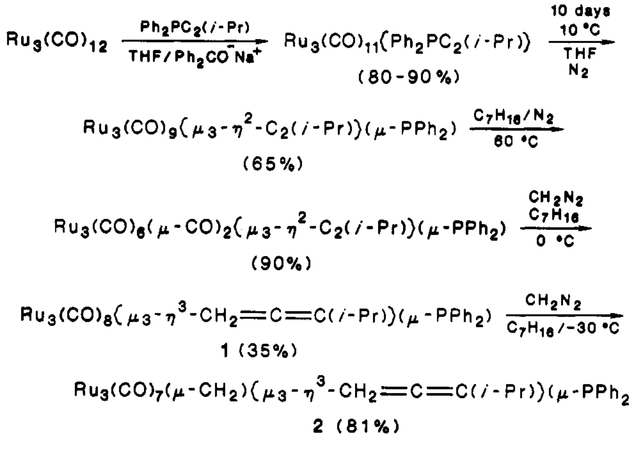

$$Ru_3(CO)_{12} \xrightarrow[\text{THF}/Ph_2CO^-Na^+]{Ph_2PC_2(i\text{-}Pr)} \underset{(80\text{-}90\%)}{Ru_3(CO)_{11}(Ph_2PC_2(i\text{-}Pr))} \xrightarrow[\substack{\text{THF}\\N_2}]{\substack{10\text{ days}\\10\ °C}}$$

$$\underset{(65\%)}{Ru_3(CO)_9(\mu_3\text{-}\eta^2\text{-}C_2(i\text{-}Pr))(\mu\text{-}PPh_2)} \xrightarrow[60\ °C]{C_7H_{16}/N_2}$$

$$\underset{(90\%)}{Ru_3(CO)_6(\mu\text{-}CO)_2(\mu_3\text{-}\eta^2\text{-}C_2(i\text{-}Pr))(\mu\text{-}PPh_2)} \xrightarrow[0\ °C]{\substack{CH_2N_2\\C_7H_{16}}}$$

$$\underset{\mathbf{1}\ (35\%)}{Ru_3(CO)_8(\mu_3\text{-}\eta^3\text{-}CH_2{=}C{=}C(i\text{-}Pr))(\mu\text{-}PPh_2)} \xrightarrow[C_7H_{16}/-30\ °C]{CH_2N_2}$$

$$\underset{\mathbf{2}\ (81\%)}{Ru_3(CO)_7(\mu\text{-}CH_2)(\mu_3\text{-}\eta^3\text{-}CH_2{=}C{=}C(i\text{-}Pr))(\mu\text{-}PPh_2)}$$

yields. Key features of this reaction[9,10] are the facile loss of CO from the 50-electron cluster $Ru_3(CO)_9${μ^3-η^2-C≡C-(*i*-Pr)}(μ-PPh_2) to give the closed 48-electron compound $Ru_3(CO)_6(\mu\text{-}CO)_2${$\mu_3$-$\eta^2$-C≡C(*i*-Pr)}($\mu$-$PPh_2$) which is highly reactive to addition of nucleophiles. This latter molecule, which behaves as if it were electronically and coordinately unsaturated, reacts rapidly, even at −78 °C, with diazomethane affording the μ_3-η^3-allenyl complex $Ru_3(CO)_8${μ_3-η^3-CH_2=C=C(*i*-Pr)}(μ-PPh_2) (**1**) which itself reacts with a second molecule of CH_2N_2 affording **2**. Conversion of **1** to **2** in the latter reaction is essentially quantitative. Important structural features of **2** are the mutual cis stereochemistry of the μ-methylene bridge across the Ru(1)–Ru(2) bond and the μ_3-allenyl unit on the Ru_3 face and the presence of an equatorial μ-PPh_2 group on the Ru(1)–Ru(3) bond.

Three main reactions involving the μ-methylene ligand have been found for **2** as shown in Scheme III. All are carbon–carbon bond forming processes, two involving coupling of the methylene unit to the unsaturated allenyl ligand while the third involves CO insertion into a metal–μ-methylene bond.

Table IV. Atomic Coordinates (Fractional × 10^4) with Esd's for $Ru_3(CO)_6(\mu\text{-}CO)(PPh_3)\{\mu_3\text{-}\eta^4\text{-}CH_2{=}C(i\text{-}Pr)CCH_2\}(\mu\text{-}PPh_2)$ (4)

atom	*x*/*a*	*y*/*b*	*z*/*c*	atom	*x*/*a*	*y*/*b*	*z*/*c*
Ru(1)	3386 (1)	8757 (1)	2505 (1)	C(17)	3970 (6)	4771 (9)	3546 (6)
Ru(2)	2874 (1)	9167 (1)	3806 (1)	C(18)	4115 (6)	4675 (10)	4309 (7)
Ru(3)	2098 (1)	9992 (1)	2411 (1)	C(19)	3845 (6)	5393 (10)	4736 (7)
P(1)	2792 (1)	7584 (2)	3126 (1)	C(20)	3439 (5)	6298 (8)	4381 (6)
P(2)	1683 (1)	11764 (2)	2070 (1)	C(21)	1956 (4)	6908 (7)	2634 (5)
O(1)	3451 (4)	7523 (7)	1100 (4)	C(22)	1472 (5)	6634 (8)	3050 (6)
O(2)	4759 (4)	7685 (6)	3319 (4)	C(23)	837 (6)	6069 (9)	2679 (6)
O(3)	2137 (4)	8624 (7)	5037 (4)	C(24)	716 (6)	5779 (9)	1944 (6)
O(4)	4315 (4)	8764 (7)	4878 (4)	C(25)	1214 (6)	6027 (10)	1530 (7)
O(5)	1289 (4)	10064 (6)	3656 (4)	C(26)	1837 (5)	6608 (9)	1883 (6)
O(6)	679 (4)	6797 (7)	1821 (6)	C(27)	782 (4)	11916 (7)	1423 (5)
O(7)	2203 (4)	9439 (7)	808 (4)	C(28)	556 (5)	11171 (8)	868 (6)
C(1)	3410 (5)	7991 (8)	1613 (5)	C(29)	−106 (6)	11321 (10)	304 (7)
C(2)	4241 (5)	8116 (7)	3002 (5)	C(30)	−518 (5)	12219 (9)	331 (6)
C(3)	2426 (5)	8848 (7)	4580 (5)	C(31)	−275 (6)	12988 (10)	896 (6)
C(4)	3774 (5)	8909 (8)	4478 (5)	C(32)	366 (5)	12814 (8)	1447 (6)
C(5)	1739 (5)	9965 (8)	3343 (5)	C(33)	2214 (4)	12553 (7)	1559 (5)
C(6)	1215 (5)	9225 (8)	2026 (6)	C(34)	2921 (6)	12688 (9)	1875 (6)
C(7)	2288 (5)	9611 (8)	1450 (6)	C(35)	3357 (6)	13317 (10)	1496 (7)
C(8)	3126 (4)	10928 (7)	3814 (4)	C(36)	3058 (6)	13746 (10)	800 (7)
C(9)	3121 (4)	10577 (6)	3071 (4)	C(37)	2340 (8)	13610 (13)	473 (9)
C(10)	3787 (4)	10490 (6)	2818 (5)	C(38)	1885 (6)	13004 (10)	847 (7)
C(11)	3780 (5)	10307 (7)	2054 (5)	C(39)	1614 (4)	12595 (7)	2870 (5)
C(12)	4507 (4)	10772 (7)	3396 (6)	C(40)	2118 (5)	13415 (9)	3172 (6)
C(13)	4549 (5)	12034 (8)	3425 (6)	C(41)	2061 (7)	14003 (10)	3827 (7)
C(14)	5173 (5)	10355 (9)	3135 (7)	C(42)	1485 (6)	13779 (10)	4149 (7)
C(15)	3302 (4)	6428 (7)	3598 (5)	C(43)	990 (5)	12981 (8)	3849 (6)
C(16)	3553 (5)	5664 (8)	3164 (6)	C(44)	1058 (5)	12403 (8)	3221 (5)

Table V. Selected Bond Lengths (Å) and Angles (deg) for $Ru_3(CO)_6(\mu\text{-}CO)(PPh_3)\{\mu_3\text{-}\eta^4\text{-}CH_2{=}C(i\text{-}Pr)C{=}CH_2\}(\mu\text{-}PPh_2)$ (4)

	(a) Bond Lengths		
Ru(1)–Ru(2)	2.826 (3)	C(1)–O(1)	1.117 (12)
Ru(1)–Ru(3)	2.880 (3)	C(2)–O(2)	1.148 (11)
Ru(2)–Ru(3)	2.788 (2)	C(3)–O(3)	1.144 (13)
Ru(1)–P(1)	2.311 (3)	C(4)–O(4)	1.122 (11)
Ru(2)–P(1)	2.301 (3)	C(5)–O(5)	1.156 (13)
Ru(3)–P(2)	2.364 (3)	C(6)–O(6)	1.135 (12)
Ru(1)–C(1)	1.888 (10)	C(7)–O(7)	1.155 (13)
Ru(1)–C(2)	1.844 (9)	C(8)–C(9)	1.415 (11)
Ru(2)–C(3)	1.867 (10)	C(9)–C(10)	1.470 (12)
Ru(2)–C(4)	1.876 (9)	C(10)–C(11)	1.402 (13)
Ru(2)–C(5)	2.350 (9)	C(10)–C(12)	1.551 (10)
Ru(3)–C(5)	1.983 (10)	C(12)–C(13)	1.566 (13)
Ru(3)–C(6)	1.917 (9)	C(12)–C(14)	1.562 (15)
Ru(3)–C(7)	1.930 (11)	P(1)–C(15)	1.823 (8)
Ru(2)–C(8)	2.234 (9)	P(1)–C(21)	1.833 (8)
Ru(2)–C(9)	2.319 (8)	P(2)–C(27)	1.841 (7)
Ru(1)–C(10)	2.303 (7)	P(2)–C(33)	1.827 (9)
Ru(1)–C(11)	2.290 (9)	P(2)–C(39)	1.813 (9)
Ru(3)–C(9)	2.154 (7)		
	(b) Bond Angles		
Ru(2)–Ru(1)–Ru(3)	58.5 (1)	C(10)–C(9)–Ru(3)	123.1 (5)
Ru(1)–Ru(2)–Ru(3)	61.7 (1)	C(9)–C(10)–C(11)	122.0 (7)
Ru(1)–Ru(3)–Ru(2)	59.8 (1)	C(9)–C(10)–C(12)	118.1 (7)
Ru(2)–Ru(1)–P(1)	52.1 (1)	C(11)–C(10)–C(12)	119.3 (8)
Ru(1)–Ru(2)–P(1)	52.4 (1)	Ru(1)–P(1)–Ru(2)	75.6 (1)
Ru(1)–Ru(3)–P(2)	137.5 (1)	Ru(1)–P(1)–C(15)	116.7 (3)
Ru(2)–Ru(3)–P(2)	130.2 (1)	Ru(1)–P(1)–C(21)	122.1 (3)
Ru(1)–C(1)–O(1)	177.2 (9)	Ru(2)–P(1)–C(15)	117.5 (3)
Ru(1)–C(2)–O(2)	177.4 (8)	Ru(2)–P(1)–C(21)	125.7 (3)
Ru(2)–C(3)–O(3)	177.5 (8)	C(15)–P(1)–C(21)	99.9 (4)
Ru(2)–C(4)–O(4)	179.3 (9)	Ru(3)–P(2)–C(27)	117.6 (3)
Ru(2)–C(5)–O(5)	127.7 (7)	Ru(3)–P(2)–C(33)	115.8 (3)
Ru(3)–C(5)–O(5)	152.1 (8)	Ru(3)–P(2)–C(39)	113.9 (3)
Ru(3)–C(6)–O(6)	176.8 (9)	C(27)–P(2)–C(33)	100.3 (4)
Ru(3)–C(7)–O(7)	161.2 (9)	C(27)–P(2)–C(39)	101.9 (4)
C(8)–C(9)–Ru(3)	114.7 (6)	C(33)–P(2)–C(39)	105.5 (4)
C(8)–C(9)–C(10)	121.6 (7)		

Scheme III

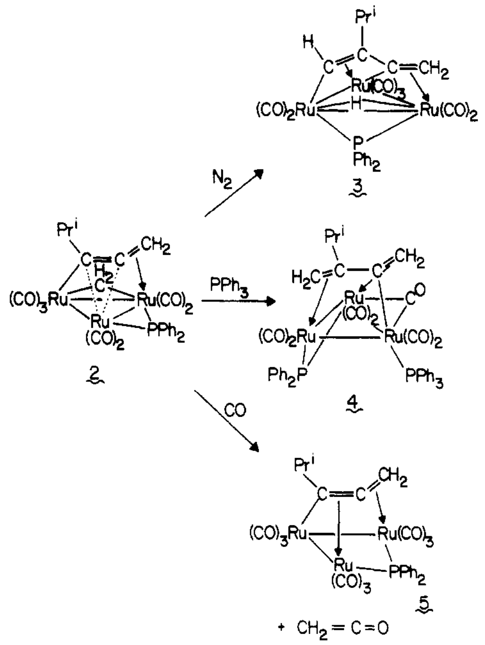

$(\mu\text{-H})Ru_3(CO)_7\{\mu_3\text{-}\eta^4\text{-}CH{=}C(i\text{-}Pr)C{=}CH_2\}(\mu\text{-}PPh_2)$ (3). In nonpolar solvents under an atmosphere of nitrogen the μ-methylene complex **2** undergoes spontaneous decomposition to afford **3** as the principal product. The IR spectrum of **3** shows only terminal ν(CO) bands. The ^1H NMR spectrum exhibits a doublet at high field (δ −18.4 ppm) typical of a hydrido bridge coupled to phosphorus (J_{PH} = 22 Hz). Singlets at 4.5 and 8.3 ppm are assigned to methylene (CH_2) and methyne (CH) groups. To confirm the origin of the hydride and the methyne CH fragment, the precursor **2** was synthesized from **1** and CD_2N_2,[11b] isolated, and converted to **3** in *n*-heptane. The ^1H NMR spectrum of this deuteriated product showed no hydride resonance at −18.4 ppm and the disappearance of the methyne resonance at 8.3 ppm but showed retention of the methylene resonance at 4.5 ppm. This experiment confirms unambiguously that the μ-CH_2 group of **2** is the source of the hydride and the methyne hydrogen atom. The assignment of ^{13}C resonances in the ^{13}C spectrum of **3** is based on comparisons with spectral features of **1** and

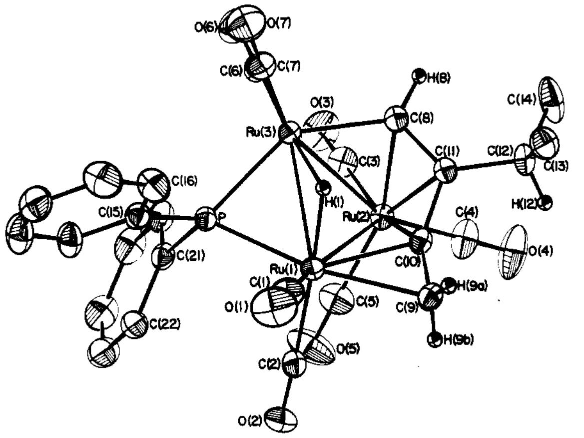

Figure 1. An ORTEP II plot of the molecular structure of (μ-H)$Ru_3(CO)_7\{\mu_3$-η^4-$CH{=}C(i\text{-}Pr)C{=}CH_2\}(\mu$-$PPh_2)$ (3). Ellipsoids are drawn at the 50% level except for hydrogen atoms which are arbitrary.

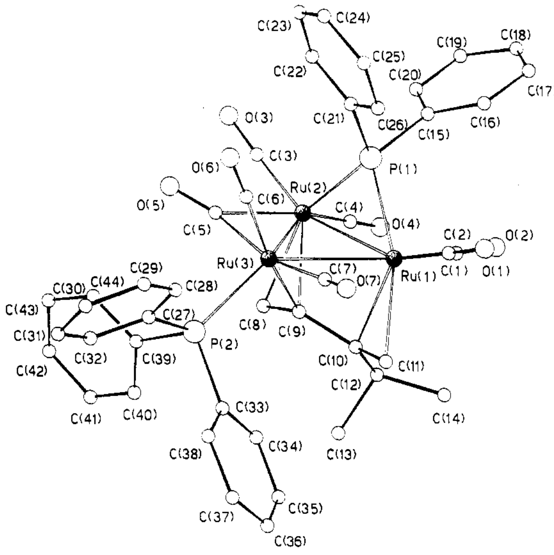

Figure 2. A perspective view of the molecule $Ru_3(CO)_6(\mu$-$CO)(PPh_3)\{\mu_3$-η^4-$CH_2{=}C(i\text{-}Pr)C{=}CH_2\}$ (4) showing the atomic numbering.

2 as well as an analysis of the magnitudes of J_{CH} coupling constants in the proton-coupled spectra. In general J_{CH} correlates well with the hybridization state of the carbon atom (cf. Figure 1): values for the sp^3 carbon atoms of the isopropyl group are 126–129 Hz; C(9) which is sp^2-hybridized has J_{CH} of 164 Hz and C(8), the methyne carbon, has an intermediate J_{CH} value (150 Hz) indicative of s character lying between sp^2 and sp^3. These results and their implications for the bonding of the hydrocarbon fragment in 3 are discussed below in the light of the X-ray data.

X-ray Crystal Structure of 3. The cluster (Figure 1) consists of a slightly asymmetric triangle of metal atoms with Ru–Ru bond lengths (2.9306 (2)–2.7534 (2) Å) in the normal range for single bonds.[16] The shortest (Ru(1)–Ru(3)) edge is bridged by both hydrido (Ru(1)–H(1) = 1.69 (5) Å, Ru(3)–H(1) = 1.74 (5) Å) and phosphido bridges (Ru(1)–P–Ru(3) = 72.4 (0)°). The hydrocarbon ligand interacts with the cluster via the four carbon atoms C(8), C(11), C(10), and C(9), of which C(9)–C(10)–C(11) constitute the original allenyl fragment in 2 and C(8) is the methyne unit derived from the μ-CH_2 group of 2, now coupled to C(11). The bond lengths C(9)–C(10) (1.369 (5) Å) and C(8)–C(11) (1.405 (4) Å) suggest substantial double-bond character, with the C(10)–C(11) bond (1.444 (4) Å) somewhat longer. The shortest Ru–C bonds to the hydrocarbon are Ru(3)–C(8) (2.075 (3)Å) and Ru(2)–C(10) (2.094 (3) Å), with the remaining distances lying in the range 2.193 (3)–2.350 (3) Å. On the basis of these observations and with use of simple electron bookkeeping, the unsaturated ligand is best described as providing a total of six electrons to the cluster. The bonding of the ligand to the Ru_3 framework lies somewhere between the extremes of the two canonical forms A and B (Figure 3). Structure A can be described as an isopropyl-substituted buta-1,3-dienediyl complex whereas form B presents the ligand as a one-electron donor from C(8), a three-electron allyl like η^3-interaction via C(8)–C(10)–C(11), and an η^2-π-olefin bond through C(9)–C(10). Support for a ground-state configuration represented by A derives from the strong Ru(2)–C(10) interaction and the asymmetry in the C(8)–C(11)–C(10) system with C(8)–C(11) notably shorter than C(11)–C(10). However, B is favored by the long C(8)–C(11) bond (1.405 (4) Å) compared to values in coordinated olefins[17] (~1.34 Å) and the residual multiple-bond character in C(10)–C(11) (1.444 (4) Å). The ^{13}C NMR data (vide supra) support the view that a model intermediate between A and B, with C(9)–C(10) as an olefinic linkage and C(8) having more sp^3 character, is appropriate.

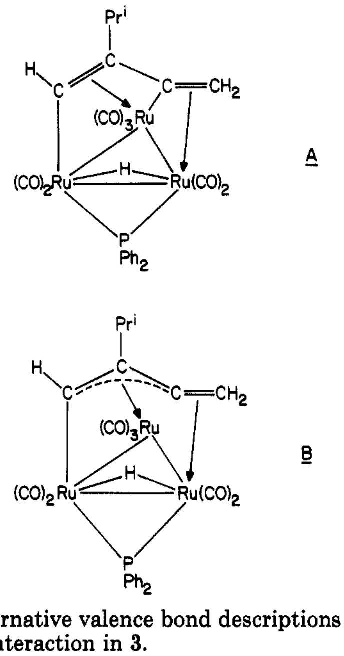

Figure 3. Alternative valence bond descriptions of the hydrocarbyl–metal interaction in 3.

Comments on the Isomerization of 2 to 3. The net overall reaction in the conversion of 2 to 3 involves cleavage of a μ-methylene C–H bond and insertion of a methyne unit into an Ru–C bond. Thus the characterization of 3 provides a rare example of carbon chain extension via coupling of a methyne fragment and an unsaturate.[1,6] Of equal significance is the demonstration that cluster-mediated C–C bond forming reactions, in this case converting an η^2-acetylide into a η^4-bound butadienediyl organic moiety via successive one carbon additions, are facile and occur under mild conditions.

A plausible mechanism for the isomerization of 2 to 3 is via the initial transfer of the μ-CH_2 moiety from the Ru(1)–Ru(3) edge of 2 onto the allenyl group generating

---

(16) Churchill, M. R.; Hollander, F. J.; Hutchinson, J. P. *Inorg. Chem.* **1977**, *16*, 2655.

(17) Ittel, S. D.; Ibers, J. A. *Adv. Organomet. Chem.* **1976**, *14*, 33.

a coordinatively and electronically unsaturated η^4-butadienyl fragment analogous to that found in the reaction of **2** with triphenylphosphine (vide infra). In the absence of a coordinating nucleophile this intermediate, to satisfy its unsaturation, could activate a C–H bond of the new hydrocarbyl to afford the μ-hydrido complex **3**. Alternatively C–H activation and cleavage, prior to methylene transfer onto the hydrocarbyl ligand, generating a μ-hydrido, μ-alkylidyne intermediate which subsequently undergoes C–C coupling to the allenyl fragment, is possible. There are precedents for aspects of both of these mechanisms. Shapley and co-workers[7] have reported a similar C–C coupling, C–H activation sequence, albeit under more severe conditions, in the thermal conversion of $Os_3(CO)_9(\mu_3\text{-}\eta^2\text{-}PhC_2Ph)(\mu\text{-}CH_2)$ to $(\mu\text{-}H)Os_3(CO)_9(\mu_3\text{-}\eta^3\text{-}PhCC(Ph)CH)$. Transfer of methylene units onto the μ-η^2-alkyne in binuclear $(\eta^5\text{-}C_5H_5)_2Ru_2(\mu\text{-}CO)(\mu\text{-}\eta^2\text{-}C_2Ph_2)$ has also been reported by Knox et al.[18] Activation and oxidative insertion into cluster-bound C–H bonds of a (μ-methyl)triosmium cluster has been described[19] as has the conversion of μ-methylene to μ-methylidyne clusters.[8a] Finally we note that there are numerous examples of binuclear μ-alkylidene complexes which on pyrolysis afford olefins via the apparent coupling of intact μ-CHR ligands.[6p]

Of the two mechanisms above, we favor the former, i.e., transfer of the μ-CH_2 group onto the hydrocarbyl prior to C–H oxidative addition, on the basis that the putative intermediate is ostensibly trapped in the presence of Ph_3P (vide infra). However, since phosphido-bridged clusters of the type discussed herein, including $Ru_3(CO)_6(\mu\text{-}CO)_2\{\mu_3\text{-}\eta^2\text{-}C{\equiv}C(i\text{-}Pr)\}(\mu\text{-}PPh_2)$ and **1**, are readily converted to 50-electron compounds via Lewis base addition and Ru–Ru bond cleavage, we cannot rule out the possibility of initial μ-CH_2 activation generating a 50-electron μ-hydrido, μ-alkylidyne complex which then reverts to the 48-electron cluster **3** via C–C coupling.

$Ru_3(CO)_6(\mu\text{-}CO)(PPh_3)\{\mu_3\text{-}\eta^4\text{-}CH_2{=}C(i\text{-}Pr)C{=}CH_2\}(\mu\text{-}PPh_2)$ (4). The reaction of **2** with PPh_3 was carried out in an effort to trap a μ-ketenyl intermediate in the synthesis of ketene from **2** and CO. The major product of this reaction was a yellow complex whose ^{31}P NMR spectrum consisted of two singlets at 35.8 (PPh_3) and 142.4 ppm (μ-PPh_2) indicative of a structure with a μ-PPh_2 group across an Ru–Ru bond[20] and a phosphine on the remaining ruthenium atom. There was no IR evidence for a ν(C=O) band near 1570 cm^{-1} for the anticipated μ-ketene[21] nor for the μ-CH_2 group of the precursor **2**. The molecular structure was determined by single-crystal X-ray analysis (Figure 2). In the Ru_3 framework the metal–metal distances fall within the narrow range 2.788 (2)–2.880 (2) Å with the shortest edge Ru(2)–Ru(3) bridged asymmetrically (Ru(2)–C(5) = 2.350 (9) Å, Ru(3)–C(5) = 1.983 (10) Å) by a carbonyl group. The dihedral angle between the planes Ru(2)–Ru(3)–C(5) and Ru(1)–Ru(2)–Ru(3) is 168.6 (3)°. The phosphido bridge on Ru(1) and Ru(2) occupies axial coordination sites [the dihedral angle between planes Ru(1)–Ru(2)–P(1) and Ru(1)–Ru(2)–Ru(3) is 103.8°] in contrast to its predecessor where the μ-PPh_2 group is equatorial. The triphenylphosphine is coordinated to Ru(3), the unique metal not spanned by the phosphido bridge, as suggested by ^{31}P NMR data.

Scheme IV

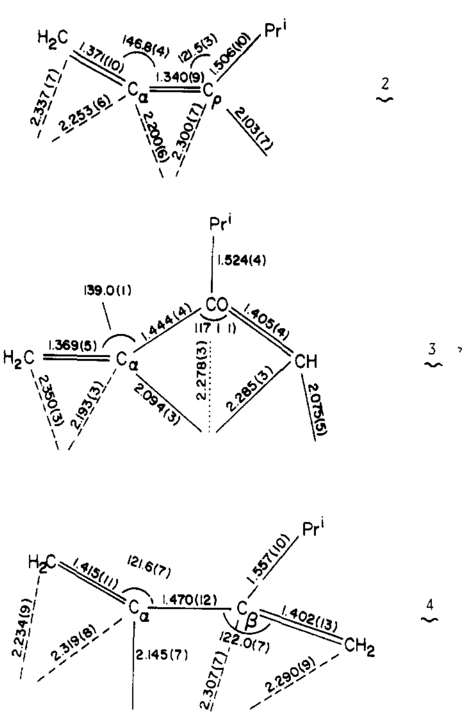

The fragment of particular interest is the unsaturated hydrocarbon which interacts with all three ruthenium atoms via a σ-bond to Ru(3) (Ru(3)–C(9) = 2.154 (7) Å) and two η^2-interactions to Ru(1) and Ru(2). The new organic ligand is derived from the allenyl and μ-methylene fragments in **2** with the methylene carbon atom C(8) now bonded to C(9). The butadienyl skeleton is only roughly planar with atomic deviations from the mean plane passing through C(8), C(9), C(10), and C(11) being 0.059 (8), −0.044 (7), −0.047 (8), and 0.061 (9) Å, respectively. The bond lengths in the butadienyl moiety and the Ru–C distances confirm that double bonds between C(8)–C(9) and C(10)–C(11) act as 2-electron donors to Ru(2) and Ru(1), respectively. Thus with the C(9)–Ru(3) σ-bond, the unsaturated fragment behaves as a 5-electron donor and is best described as a 2-isopropyl-1,3-butadien-3-yl ligand. There is an interesting comparison with the closely related butadien-diyl moiety in **3** formed via methyne transfer to the β-carbon of the original acetylide and also with the η^3-allenyl ligand in the precursor **2** (Scheme IV), all three of these groups being attached to a similar closed Ru_3 skeleton. Scheme IV illustrates quite clearly that the η^2-coordinated $>C_\alpha{=}CH_2$ moiety is remarkably similar in all three compounds while the central C_α–C_β bond undergoes substantial lengthening from 1.340 (9) Å in **2** to 1.470 (12) Å in **4**. The trans stereochemistry of the diene fragments in **3** and **4** appears to be the direct result of a cis transfer from the metal to the carbon atom of the allene bearing the isopropyl substituent.

Reaction of the μ-Methylene Complex 2 with CO: Formation and Trapping of Ketene. Complex **2** reacts with CO in the absence of methanol to give the 50-electron open-edged allenyl cluster $Ru_3(CO)_9\{\mu_3\text{-}\eta^3\text{-}CH_2{=}C{=}C(i\text{-}Pr)\}(\mu\text{-}PPh_2)$ (**5**) which is also the product of direct CO addition to $Ru_3(CO)_8\{\mu_3\text{-}\eta^3\text{-}CH_2{=}C{=}C(i\text{-}Pr)\}(\mu\text{-}PPh_2)$, described in the first paper in this series.[9] The characterization of **5** and an account of the chemistry of $Ru_3(CO)_8\{\mu_3\text{-}\eta^3\text{-}CH_2{=}C{=}C(i\text{-}Pr)\}(\mu\text{-}PPh_2)$ are given in the following paper. In the presence of methanol **2** and CO

---

[18] Colborn, R. E.; Dyke, A. F.; Knox, S. A. R.; MacPherson, K. A.; Orpen, A. G. *J. Organomet. Chem.* **1982**, *239*, C15.

[19] (a) Calvert, R. B.; Shapley, J. R. *J. Am. Chem. Soc.* **1977**, *99*, 5225. (b) Calvert, R. B.; Shapley, J. R. *J. Am. Chem. Soc.* **1978**, *100*, 7726.

[20] See for example: (a) Carty, A. J.; MacLaughlin, S. A.; Taylor, N. J. *J. Organomet. Chem.* **1981**, *204*, C27. (b) Carty, A. J. *Adv. Chem. Ser.* **1981**, *No. 196*, 163. (c) Duttera, M. R.; Geoffroy, G. L.; Novotnak, G. C.; Roberts, D. A.; Shulman, P. M.; Steinmetz, G. R. *Organometallics* **1982**, *1*, 1008.

[21] Roger, M.; Keim, W.; Strutz, H. *J. Organomet. Chem.* **1981**, *219*, C5.

Scheme V

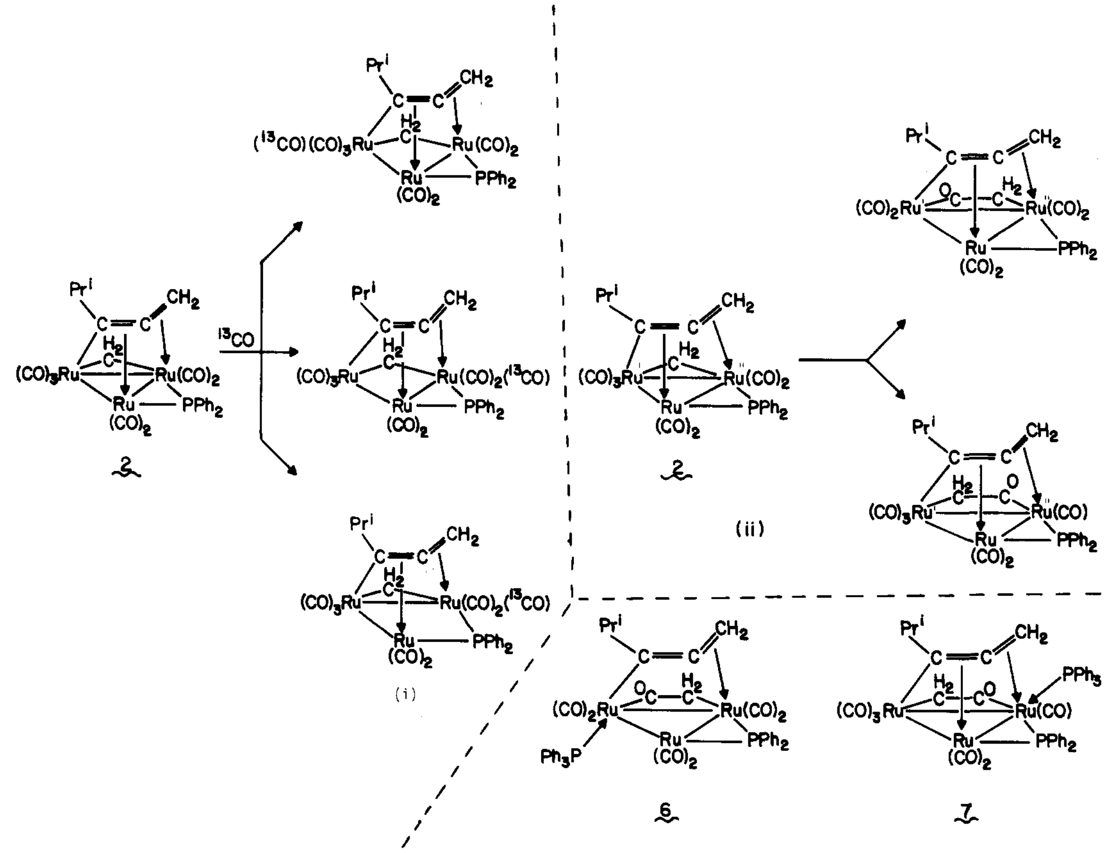

yield 5 and methyl acetate. The latter was identified by its IR spectrum (ν(C=O) 1752 cm^{-1}) which corresponded to that of an authentic sample and by ^{13}C-labeling experiments using $^{13}CH_3OH$. The expected product $^{13}CH_3OCOCH_3$ was confirmed by ^{13}C and ^{1}H NMR spectroscopy. The ^{13}C spectrum exhibited two AX quartets at 50.98 and 50.25 ppm with J_{CH} = 146 and 140 Hz, identical with that of an authentic sample. These results can be explained by involving the formation of "CH$_2$CO" either coordinated to the cluster or as free ketene. The formation of 5, even in the absence of CH$_3$OH, tends to suggest the release of free ketene. The insertion of CO into a methylene metal bond to generate a ketenyl ligand and subsequently ketene is not unprecedented, but very few examples have been reported for polynuclear systems. Keim et al.[21] observed the formation of methyl acetate from CH$_3$OH-spiked solutions of $Fe_2(CO)_8(\mu\text{-}CH_2)$ with concurrent destruction of the organometallic components. The non metal–metal bonded complex $[\eta^5\text{-}C_5H_5Ru(CO)_2]_2(\mu\text{-}CH_2)$ also gives CH$_3$OCOCH$_3$ in the presence of CO.[22] In both cases ketenyl intermediates were implicated as intermediates. A model μ-ketenyl cluster, $Os_3(CO)_{12}(\mu\text{-}CH_2CO)$, has been fully characterized by Geoffroy and co-workers[8c] as the product of the addition of two molecules of CO to $Os_3(CO)_{11}(\mu\text{-}CH_2)$. The bridging diphenylcarbene ligand in $(\eta^5\text{-}C_5H_5)_2Mo_2(CO)_4(\mu\text{-}CPh_2)$ affords Ph$_2$C=C=O under an atmosphere of CO.[23] There are also numerous examples of the synthesis of "free" or coordinated ketenes from mononuclear carbenes and CO.[24] More recently, abstraction of hydrogen from a metal-bound acetyl group, forming ketene, has been reported.[25] In all of the reported examples of CH$_2$=C=O formation from bridging methylenes, CO insertion[26] into an M–CH$_2$–M system has been implicated. We thus sought to establish the stoichiometry of the reaction, the origin of the "inserting" CO, and to trap the supposed ketenyl intermediate.

Complex 2 reacts with CO in the presence of methanol to give 5 and methyl acetate as described by eq 1. The

$$Ru_3(CO)_7(\mu\text{-}CH_2)\{\mu_3\text{-}\eta^3\text{-}CH_2{=}C{=}C(i\text{-}Pr)\}(\mu\text{-}PPh_2) + 3CO + CH_3OH \rightarrow Ru_3(CO)_9\{\mu_3\text{-}\eta^3\text{-}CH_2{=}C{=}C(i\text{-}Pr)\}(\mu\text{-}PPh_2) + CH_3OCOCH_3 \quad (1)$$

reaction can be readily monitored by a combination of ^{1}H, ^{31}P, and ^{13}C NMR; 2 and 5 have ^{31}P shifts differing by 162.3 ppm, and $^{13}CH_3OCOCH_3$ is detected by its characteristic ^{1}H and ^{13}C shifts as described earlier. Isotopic labeling studies using *both* $^{13}CH_3OH$ and ^{13}CO gave only $^{13}CH_3OC(O)CH_3$ and not $^{13}CH_3O^{13}C(O)CH_3$.[27] This result establishes unequivocally that the CO which inserts into the μ-methylene bridge to give ketene must be one of the original coordinated CO molecules of 2 and is not derived from external CO. A similar conclusion was drawn by Geoffroy and co-workers for ketene derived from $Os_3(CO)_{11}(\mu\text{-}CH_2)$.[8c] Since direct intermolecular attack on coordinated –CH$_2$– by CO is ruled out, the two likely pathways for insertion of CO into the Ru–CH$_2$–Ru system are (i) and (ii) in Scheme V. Mechanism (i) involves an associative addition to 2 with Ru–Ru bond cleavage giving

---

(22) Lin, Y. C.; Calabrese, J. C.; Wreford, S. S. *J. Am. Chem. Soc.* **1983**, *105*, 1679.

(23) Messerle, L.; Curtis, M. D. *J. Am. Chem. Soc.* **1980**, *102*, 7789.

(24) For a summary of these reactions see: (a) Fischer, E. O. *Adv. Organomet. Chem.* **1976**, *14*, 18. (b) Herrmann, W. A.; Plank, J. *Angew. Chem., Int. Ed. Engl.* **1978**, *17*, 525.

(25) Hommeltoft, S. I.; Baird, M. C. *J. Am. Chem. Soc.* **1985**, *107*, 2548.

(26) There is no intent here to differentiate insertion of CO into a μ-methylene–metal bond and μ-methylene migration to coordinated CO.

(27) $^{13}CH_3O^{13}C(O)CH_3$ has a ^{13}C resonance at 170.4 ppm due to the carbonyl carbon atom. This resonance was absent in the labeled methylacetate produced from 2, $^{13}CH_3OH$, and ^{13}CO.

Scheme VI

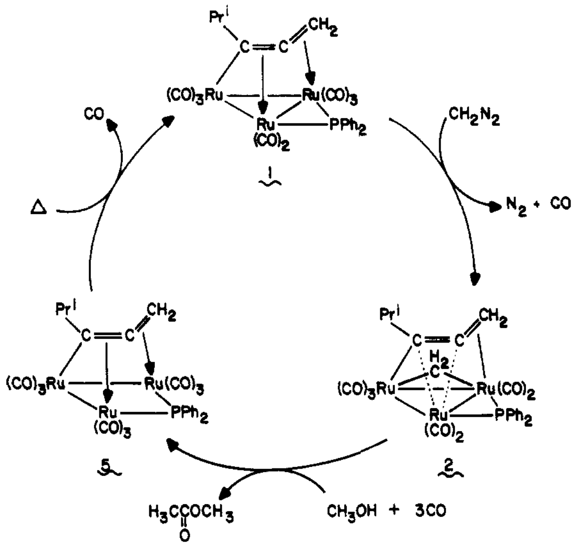

a 50-electron species and supposes that there is either site specific incorporation of nonlabeled CO or that the low statistical probability of labeled ^{13}CO inserting into the bridge effectively precludes identification of carbonyl-labeled $CH_3O^{13}C(O)CH_3$. In pathway (ii) initial intramolecular CO insertion into one arm of the methylene bridge affords a 46e cluster which subsequently adds ^{13}CO. The two mechanisms differ from those of Geoffroy[8c] in that the inherent symmetry of the osmium system does not distinguish which metal supplies the carbonyl for insertion. In principle the asymmetry of 2 would allow a differentiation between the two sources, labeled Ru′ and Ru″ in Scheme V(ii), if the intermediate ketenyl complex could be isolated. Since only the 50-electron allenyl complex 5 was detected under CO, no ketenyl intermediate being spectroscopically evident, an obvious experiment was to react 2 in the presence of 1 equivalent of a Lewis base in an attempt to intercept and trap one of the two clusters 6 and 7 (Scheme V) which should be readily distinguishable by their ^{31}P NMR characteristics. Reaction of 2 with PPh_3 did not unfortunately give the anticipated ketenyl complex. Instead, as described earlier, the major product, 4, arose via transfer of an intact CH_2 group onto the hydrocarbyl.

Despite the failure to intercept a ketenyl intermediate, there is ample evidence from product identification and stoichiometric reactions to establish a cycle involving 1, 2, and 5 in the synthesis of ketene (Scheme VI). The allenyl cluster 1 reacts with CH_2N_2 in high yield affording the μ-methylene cluster 2 which in turn is converted stoichiometrically in the presence of 3 equivalents of CO and methanol to methyl acetate and 5. Cluster 5 reconverts slowly via loss of CO on purging with N_2 to 1. Although this cycle is closed, it does not at present represent a feasible system for the catalytic synthesis of ketene since the back reaction of 1 with CO is rapid whereas loss of CO from 5 is slow and CH_2N_2 does not react at all with the 50-electron species 5. We are currently attempting to influence the relationship between 48-electron 1 and 50-electron 5 in favor of 1 by changing the phosphido bridge and the allenyl substituent.

Conclusion

The chemistry described in this paper for 2 has revealed a number of interesting new aspects of the behavior of μ-methylene ligands in clusters. Of specific note are facile CH_2 and CH transfers onto unsaturated hydrocarbyl ligands and a new example of ketene generation via CO–methylene coupling. These results provide further evidence that μ-methylene ligands in clusters have a versatile and intriguing chemistry.

Acknowledgment. This research was supported by the Natural Sciences and Engineering Research Council of Canada via operating grants to A.J.C. and a scholarship to D.N.

Registry No. 1-d_2, 110570-41-7; 2, 87829-54-7; 2-d_2, 87829-55-8; 2-d_4, 110589-07-6; 3, 87829-52-5; 4, 110570-43-9; 5, 110570-42-8.

Supplementary Material Available: Listings of anisotropic thermal parameters (Tables S1, S4) and remaining bond lengths and angles (Tables S2, S5) for complexes 3 and 5 (5 pages); listing of structure factors (Tables S3, S6) for complexes 3 and 5 (56 pages). Ordering information is given on any current masthead page.